ChemComm

Accepted Manuscript

Journal Name

COMMUNICATION

High-Yield Photolytic Generation of Brominated Single-Walled Carbon Nanotubes and their Application for Gas Sensing

D. Hines,[a] M. H. Rümmeli,[b,c] D. Adebimpe*[d] and D. L. Akins*[,a]

We present a facile and efficient photobromination technique for the covalent sidewall functionalization of SWNT using N-bromosuccinamide as the bromine source. The modified bromine functionalized SWNTs are used as active agents in a resistance measuring electrode system for sensing and discrimination of analyte vapors.

Single-walled carbon nanotubes (SWNTs) are exciting candidates to use as active constituents in devices and sensors because of their nanoscale dimensions, high aspect ratios, large specific surface areas, and outstanding mechanical and electronic properties.[1-8] However, use of SWNTs for actual applications in devices and sensors has proven problematic due to their intrinsic chemical inertness, the difficulty to control their chirality (which imbues them with semiconductor or metallic electronic properties), and especially their extremely low solubility in most common solvents. Other researchers have attempted to fine-tune the properties of carbon nanotubes through chemical functionalization in order to overcome the solubility challenge.[9, 10] In general, it has been found that chemical functionalization of carbon nanotubes for solubility purposes also impacts chemical interaction specificity and sensitivity, as well as significantly alters a nanotube's physical, electronic and optical properties.[3] Such alterations, in fact, can enhance the application potential for nanotubes as active agents in sensors and devices.[11-20]

In this paper, we report results for an initial effort (with bromine atoms as the SWNTs adduct) that we have undertaken to modify the interaction affinity of SWNTs for sensing of a number of single component analyte vapors. Subsequent efforts will deal with other covalent adducts, with the aim of creating a finger-print response matrix for a given vapor component in a multicomponent vapor with the various covalently modified SWNT coated electrodes. The sensing system that we seek to develop would be able to measure, with high accuracy, the fractional composition of the various components in a complex vapor, thus aiding in identifying the source of the vapor. Such a system is broadly referred to as an e-nose.

Efforts at developing CNT-based gas sensors have centered primarily on two approaches to transduce an analyte's signal (e.g., concentration) directly into an electrical signal. One involves incorporation into a chemical field-effect transistor (ChemFET) configuration. The second involves creation of a chemical resistor (Chemiresistor) element. In the ChemFET configuration the CNT or an ensemble of CNT are electrically contacted across a source and drain. The conductance across the CNT is then modulated using a gate, where, in essence, the gate is a third electrode capacitively coupled through a thin dielectric layer to the CNT or CNT ensemble.

In the Chemiresistor configuration, the conductance of a single tube or an ensemble is measured across two electrodes. Obviously, creation of a Chemiresistor is simpler and cheaper to produce, as well as requires less complex ancillary electronics to operate.[21] Both the Chemiresistor and ChemFET configurations can operate with either pristine or functionalized tubes. However, as mentioned vide supra, the use of functionalized tubes can lead to improved sensing performance since, for example, the chemical affinity can be tuned to enhance sensitivity. The two main surface functionalization approaches for CNTs involve noncovalent or covalent interactions. Noncovalent functionalization is typically based on supramolecular complexation through van der Waals, electrostatic and π-stacking interactions, that result in surface adsorption of molecules.[22, 23] Covalent functionalization of CNT, as the name suggests, involves a covalent bond between the CNT and the molecule or atom being attached, and is hence the more stable functionalization approach.

Typically, covalent functionalization is achieved by the esterification or amidation of carboxylic acid groups.[24-26] Another useful functionalization strategy involves creation of halogen radicals.[27, 28] Usually the functionalization of carbon nanotubes with halogens is achieved by oxidizing F_2 gas,[29-31] followed by electrochemical treatment with Br_2 and Cl_2,[32] or using elemental iodine through a modified Hunsdiecker-type reaction.[33] Functionalization with halogens, which are electron-withdrawing entities, leads to the formation of carbon-halogen bonds, which create defect sites in the sidewalls of CNTs, resulting mainly in changes in the tubes' electronic properties.[34] For example, Bahr et al.[35] reported changes

in the electronic conductivity of fluorine-functionalized SWNTs; they found a resistance > 20 MΩ as compared to 10 - 15 Ω for pristine SWNT.

In terms of bromine-based functionalization of CNT, the literature is quite sparse. A small number of publications have reported the bromination of the sidewall of a carbon nanotube. Mazov *et al.*[36] have reported studies on multiwall CNT halogenation by means of direct vapor-phase bromination, and demonstrated a 2.5 wt.% yield. Colomer *et al.*[27] have reported studies dealing with the bromination of doubled-walled carbon nanotubes through the use of a microwave-assisted, bromination technique. Higher yields of between 30 and 40 wt % can be obtained by the direct chemical vapour deposition synthesis of nanotubes.[37]

To our knowledge, no studies have been reported that utilize photobromination to form bromine radicals from N-bromosuccinamide to promote the addition of bromine to the sidewall of SWNTs. Here, in pursuit of developing a platform for chemical sensing, we have identified a facile and efficient photobromination technique for the covalent sidewall functionalization of SWNT with bromine. In this process the radiation source cleaves the bromine molecule into radicals by photolysis. The generated free radicals can then be expected to attack the CNT wall much like radicals do in diazotization that leads to conjugation with benzene.[35] The process is illustrated in Scheme 1 below.
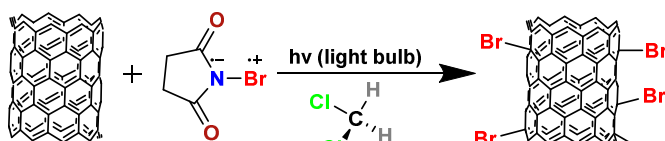
Scheme 1: Formation of brominated SWNT using N-bromosuccinamide (N-BROMOSUCCINIMIDE) for bromine radical formation via photolysis in dichloromethane.

Remarkably high functionalization yields of between 15 - 25 wt.% are found for this photolysis reaction. In so far as we are aware this is the highest post-synthesis bromination yield obtained. Herein, the as-produced brominated SWNT have been used as active agents for electronic nose-type (e-Nose) applications aimed at vapor compositional analysis (i.e., vapor analysis).

Poly-brominated-SWNT nanotubes were fabricated by photolytic decomposition of N-bromosuccinamide (yellow in color) in the presence of pristine nanotubes. Typically, 20 mg of the SWNT sample was sonicated in 15 mL of dichloromethane for 20 minutes. The dispersed mixture was then poured into a 100 mL round bottom flask. N-bromosuccinamide (11 mg) was then added, which resulted in the formation of a dark orange-color dispersion. The dispersion was then refluxed while irradiated through the bottom of the flask with light from a conventional 100 watt incandescent light bulb (General Electric, A19 incandescent bulb). Exposure of the dispersion to the radiation promotes the formation of free bromine radicals. The reaction was allowed to run for about 15 minutes during which time out-gassing of gaseous components (oxides of nitrogen, oxides of carbon, hydrogen bromide). Then, 21 mg of N-bromosuccinamide was added to the dispersion to further drive the reaction. The reaction was allowed to continue uninterrupted for another 90 minutes, after which a bright yellow dispersion formed with a phase separated suspension on top. At this point, the radiation source was lowered below the reaction flask (from 5 mm to 40 mm) to reduce the reaction rate. The reaction was allowed to proceed for another 10 hours. For other syntheses studies, the reaction procedure

was modified by allowing the final step to occur for durations of 24 and 48 hours. In all cases, after the reaction, a light yellowish dispersion was obtained with no heterogeneous suspension. The dispersion was cooled and filtered through a PTFE membrane (0.45 μm, 25mm), and a resulting precipitate was washed thoroughly with chloroform followed by several washing with diethyl ether. The resultant product was dried overnight at 60 °C in a Napco 5861 vacuum oven.

To fabricate the gas sensors, the SWNT functionalized with bromine sample was first dispersed in mCresol (Sigma Aldrich: 98+ %)), then spin-coated onto a commercially prepared substrate consisting of an array of interdigitated, microstructured gold electrodes. The SWNT mat coated electrode apparatus was then dried at 60 °C in a conventional oven for 10 minutes. The resulting electrically contacted SWNT mat served as the active sensing element. The fabrication process is schematically represented in Figure S1 in the Supporting Information (SI) document. The experimental setup for the sensor is provided in Figure S2 (of the SI document). In essence, analytes interact with the brominated-SWNT mat through weak dispersive or chemical forces. The interactions, which are related to the surface concentration of the analyte, perturb the electronic system of the mat, resulting in resistance changes, which are monitored and recorded using a lab built PXI-platform from National Instruments (NI), Model 1042.

We compared the Raman spectra of pristine SWNTs and Br functionalized SWNTs (see panel A of Figure 1). In general, three key Raman bands are used as the finger-print pattern of sp^2 bonds in carbon materials. These are the D-band (defect) at ca. 1350 cm^{-1}, the G-band (graphitic) at ca. 1600 cm^{-1}, and the 2D-band (second-order band) at ca. 2700 cm^{-1}. These bands are observed for all our samples, but with variations between the functionalized and pristine specimens. The G-band, which exhibits a Breit-Wigner-Fano line profile, broadens and upshifts (14 cm^{-1}) upon Br functionalization. Such a change is expected with bromine functionalization of SWNTs, indicating electron transfer between Br atoms and SWNTs.[38-41] The D-band is found to increase in intensity relative to the G-band and to exhibit broadening and upshifting; the latter, as in the case of the G-band, arise from charge transfer. The increase in relative intensity exhibited by the D-band indicates a decrease in structural order of the SWNT, and can be attributes to the formation of vacancies and the loss of some sp^2 character on the nanotube's surface resulting from bond formation with the functional groups.[42] And, since the photolysis reaction is not particularly harsh, the above changes are expected to be due to bromination alone.

The radial breathing modes (RBMs), which lay between ca. 150 cm^{-1} and 300 cm^{-1}, are found to be considerably weaker after the functionalization, consistent with the impact expected when mass is attached to the nanotubes surface.

FTIR measurements also show clear differences between pristine and functionalized samples (see panel B of Figure 1). The FTIR spectrum of the pristine sample shows a band at ca. 1590 cm^{-1} that is attributable to C=C vibration. The band is slightly upshifted in the brominated sample, consistent with stiffening associated with doping. In addition, a relatively intense new band appears at ca. 650 cm^{-1}, which is attributed to a C-Br vibration[43] and suggests the successful incorporation of Br atoms to the SWNT.

 We also employed thermogravimetric analysis on samples prepared using a 24 hrs photolysis reaction period. The data was compared to the pristine samples, as shown in panel C of Figure 1. The pyrolysis was conducted in a N_2 atmosphere up to a temperature of 1000 °C. The pristine SWNT are relatively stable and thermogravimetric

analysis resulted in a weight loss of 10% at 1000 °C. In the case of the brominated SWNT samples, the weight loss rate changed significantly at ca. 210 °C, followed by a further loss at ca. 350 °C (see the derivative data in panel D of Figure 1). The weight loss between the two regions can be attributed to thermal decomposition involving Br atoms and suggests a 15 wt.% (± 2 wt.%) loss, in good agreement of the EDX data (ca. 17 wt.%). A further de-composition step occurs between 510 and 600 °C, attributable to the decomposition of the SWNT.
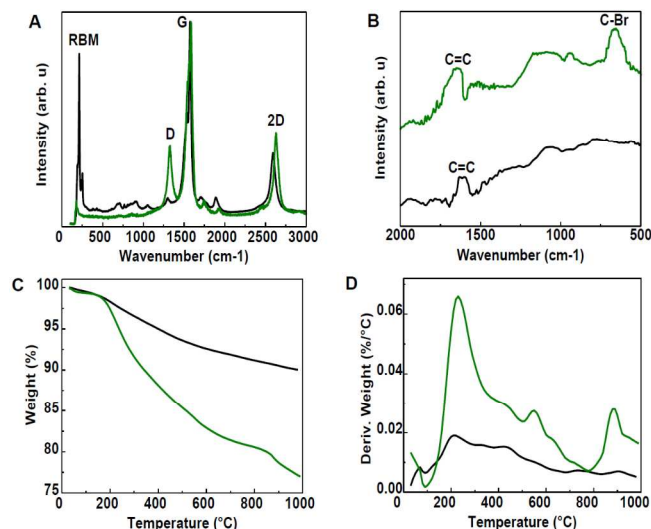

Fig. 1. Green and black traces in all panels refer to functionalized and pristine SWNT samples, respectively. (A) Raman spectra using 632-nm excitation for functionalized Br-SWNT and pristine SWNT samples. (B) FTIR-KBr spectra of samples. (C) TGA and (D) DTA measurements conducted under pure nitrogen at heating rate of 10 °C per minute for the same samples.

SEM investigations of the specimens showed no discernible differences between the pristine and Br-functionalized samples in terms of their morphology (e.g., see Figure S4A in the SI). Energy dispersive spectroscopy (EDX) was also used as this can show the level of bro-mine species present in the samples. Measurements were made for multiple samples that underwent the photolysis reaction for 12, 24 and 48 hours (Table S1); the EDX measurements indicated values of 7, 17 and 15 wt.% (± 4 wt.%), respectively. In Table S1 (see SI), the data shows that the incorporation of Br species reaches a saturation limit that does not increase for reaction times longer than 24 hrs. The above levels of Br incorporation substantially exceed previously reported values that reached yields only up to 8 wt.%.[27, 36] Because of the polar nature of halogen-carbon bonds, the hydrogen bonding capacity of halogen functionalized sp^2 carbon is improved resulting in enhanced affinity of the functionalized carbon species for aliphatic vapors or small molecular volatiles. To assess the gas sensing potential of Br-SWNT, we exposed Br-SWNT sensors to various one component vapors independently. The vapors used were HCl, NH_3, HNO_3, C_3H_6O, C_2H_3N, $C_2H_4O_2$, H_2SO_4 and N,N-dimethylacetamide. To conduct a measurement, initially, a baseline was established under a pure N_2 flow for at least 1 min. Then the sensor was exposed in periodic cycles of pure N_2 followed by carrier gas N_2 containing a selected analyte vapor and the sensor's response was measured. The sensor showed high sensitivity to the eight volatile compounds mentioned above for concentrations varying from ca. 286 to 1645 ppb. The concentrations calculated primarily from the measurement volume, specific density at 20 °C, the flow rate of the carrier gas, and molecular weights of compounds. Table S2 provides the calculated concentration for each

analyte mixture. Injection of the analyte vapor was externally controlled by a solenoid driven valve and a flow meter.

Figure 2 shows the resistance response of the brominated SWNT sensors to the various vapors. (A comprehensive set of responses for all the vapors investigated is provided Figure S5 in the SI document).
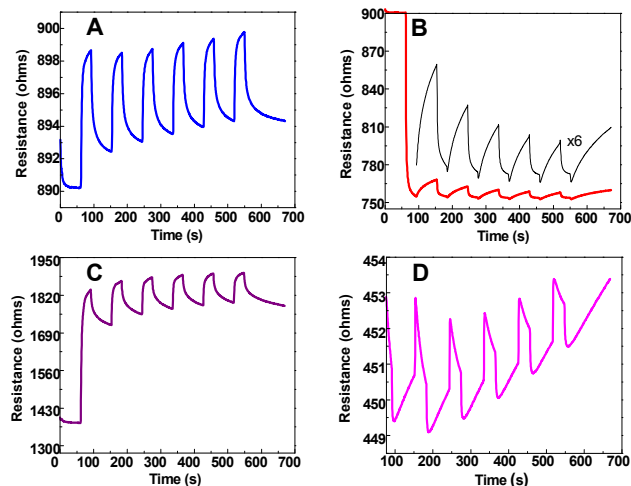

Fig. 2. Sensing profiles for the Br-SWNT coated electrodes. Analytes used for panels (A) through (D) are, respectively, ethanol, HCl, ammonia and sulfuric acid. Response data in panel B has been amplified by a factor of 6 for easier viewing, but true signal magnitude is provided by lower smaller response.

The shapes of resistance response curves differ for the various analytes. The simplest interpretation of the shape of the response to the presence or absence of analyte in the flow mixture is that adsorption build up occurs when the analyte is flowing, while when the flow of analyte is terminated, desorption occurs, as the carrier gas sweeps the analyte off of the electrode. This model suggests the possibility to differentiate between analytes based on measurement of their different response curves. Our analysis scheme is to determine the ratios of the response function areas when the analyte was present (i.e., the "on-time" area) to that when the analyte is not present (i.e., the "off-time" area) as a function of the percentage change in resistance (R); i.e., $\Delta R\% = \left((R - R_0)/R_0 \right) \times 100$, as shown in top left panel of Fig. 3.

Panel B of Figure 3 shows random response cycles area ratios for several cycles of the various response curves (for the different analytes) shown in Figure 2 and Figure S5 as a function of $\Delta R\%$. The net effect of choosing different cycles for a given analyte is to define the inherent uncertainty to be anticipated for any given measurement. Additionally, when the random cycle measurements cluster together, as depicted in panel B of Figure 3 for several of the analytes, one can conclude that if a subsequent measurement of an area ratio for a single cycle (or the average of several cycles) for an unknown analyte falls within the cluster region, then the identity of the analyte can be inferred to a high level of confidence.

To summarize, we have demonstrated a facile and efficient means of functionalizing SWNT with Br based on a UV photolysis synthesis route. The functionalization yield is significantly higher as compared to other post CNT-synthesis approaches.
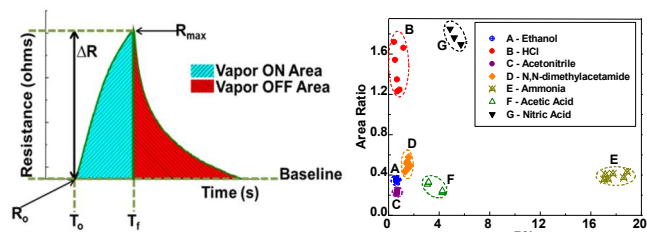
Fig. 3. Left panel represents schematic for parameters ΔR and "vapor-on" and "vapor-off" areas, whose values are used for determining parameters used in the right panel. One finds clustering of area ratios for 7 analytes vapors exposed to SWNT-bromine sensor; the dashed ellipsoids enclose suggested clusters. The vapors used were A- ethanol, B- HCl, C- acetonitrile, D- N,N-dimethylacetamide E- ammonia, F- acetic acid and G- nitric acid.

In addition, we show for the first time, that the profile of the response curves for gas chemiresistor sensors could provide a means for analyte selectivity, in other words, gas identification.

Notes and references

[a] Department of Chemistry and the Center for Analysis of Structures and Interfaces (CASI), The City College of New York and the Graduate School and University Center (CUNY), New York, NY, USA.

[b] Center for Integrated Nanostructure Physics, Institute for Basic Science (IBS), Daejon 305-701, Republic of Korea.

[c] Department of Energy Science, Department of Physics, Sungkyunkwan University, Suwon 440-746, Republic of Korea.

[d] Polymath Interscience, LLC, Annapolis, MD, USA.

† Electronic Supplementary Information (ESI) available: Schematic of brominated-SWNT decorated interdigitated electrode; vapor delivery and distribution system; AFM of SWNT-Bromine cross-linking on electrodes; SEM and EDAX data for Br-SWNT; and sensing ability of Br-SWNT gas sensor. See DOI: 10.1039/c000000x/

1. M. Dresselhaus, G. Dresselhaus and P. and Avouris, *Springer-Verlag Berlin Heidleber G.*, 2001.
2. M. Hughes, G. Z. Chen, M. S. Shaffer, D. J. Fray and A. H. Windle, *Chem. Mater.*, 2002, **14**, 1610-1613.
3. R. Saitô, G. Dresselhaus and M. Dresselhaus, *Physical properties of carbon nanotubes*, 1998.
4. A. Hirsch and O. Vostrowsky, in *Functional molecular nanostructures*, Springer, 2005, pp. 193-237.
5. R. H. Baughman, A. A. Zakhidov and W. A. de Heer, *Science*, 2002, **297**, 787-792.
6. F. Kreupl, A. P. Graham, G. S. Duesberg, W. Steinhögl, M. Liebau, E. Unger and W. Hönlein, *Microelectron. Eng.*, 2002, **64**, 399-408.
7. C. Cantalini, L. Valentini, I. Armentano, J. M. Kenny, L. Lozzi and S. Santucci, *J. Eur. Ceram. Soc.*, 2004, **24**, 1405-1408.
8. J. Suehiro, G. Zhou, H. Imakiire, W. Ding and M. Hara, *Sens. Actuators, B*, 2005, **108**, 398-403.
9. R. J. Chen, S. Bangsaruntip, K. A. Drouvalakis, N. W. S. Kam, M. Shim, Y. Li, W. Kim, P. J. Utz and H. Dai, *P NATL ACAD SCI*, 2003, **100**, 4984-4989.
10. D. Tasis, N. Tagmatarchis, A. Bianco and M. Prato, *Chem. Rev.*, 2006, **106**, 1105-1136.
11. F. Lu, L. Gu, M. J. Meziani, X. Wang, P. G. Luo, L. M. Veca, L. Cao and Y. P. Sun, *Adv. Mater.*, 2009, **21**, 139-152.
12. A. Bianco, K. Kostarelos and M. Prato, *Curr. Opin. Chem. Biol.*, 2005, **9**, 674-679.
13. M. Prato, K. Kostarelos and A. Bianco, *Acc. Chem. Res.*, 2007, **41**, 60-68.
14. O. Zhou, H. Shimoda, B. Gao, S. Oh, L. Fleming and G. Yue, *Acc. Chem. Res.*, 2002, **35**, 1045-1053.
15. R. Raffaelle, B. Landi, J. Harris, S. Bailey and A. Hepp, *Mater. Sci. Eng., B*, 2005, **116**, 233-243.
16. W. Bauhofer and J. Z. Kovacs, *Compos. Sci. Technol.*, 2009, **69**, 1486-1498.
17. J. N. Coleman, U. Khan, W. J. Blau and Y. K. Gun'ko, *Carbon*, 2006, **44**, 1624-1652.
18. K. LeeáTan, *J. Mater. Chem.*, 2001, **11**, 2378-2381.
19. K. Santhanam, R. Sangoi and L. Fuller, *Sens. Actuators, B*, 2005, **106**, 766-771.
20. J. Kong, M. G. Chapline and H. Dai, *Adv. Mater.*, 2001, **13**, 1384-1386.
21. T. Zhang, S. Mubeen, N. V. Myung and M. A. Deshusses, *Nanotechnology*, 2008, **19**, 332001.
22. A. Star, J. F. Stoddart, D. Steuerman, M. Diehl, A. Boukai, E. W. Wong, X. Yang, S. W. Chung, H. Choi and J. R. Heath, *Angew. Chem. Int. Ed.*, 2001, **40**, 1721-1725.
23. H. Xia, Q. Wang and G. Qiu, *Chem. Mater.*, 2003, **15**, 3879-3886.
24. J. Chen, M. A. Hamon, H. Hu, Y. Chen, A. M. Rao, P. C. Eklund and R. C. Haddon, *Science*, 1998, **282**, 95-98.
25. M. A. Hamon, H. Hu, P. Bhowmik, S. Niyogi, B. Zhao, M. E. Itkis and R. C. Haddon, *Chem. Phys. Lett.*, 2001, **347**, 8-12.
26. J. E. Riggs, Z. Guo, D. L. Carroll and Y.-P. Sun, *J. Am. Chem. Soc.*, 2000, **122**, 5879-5880.
27. J.-F. Colomer, R. Marega, H. Traboulsi, M. Meneghetti, G. Van Tendeloo and D. Bonifazi, *Chem. Mater.*, 2009, **21**, 4747-4749.
28. F. Lu, Rochester Institute of Technology, 2010.
29. V. N. Khabashesku, W. E. Billups and J. L. Margrave, *Acc. Chem. Res.*, 2002, **35**, 1087-1095.
30. H. Muramatsu, Y. Kim, T. Hayashi, M. Endo, A. Yonemoto, H. Arikai, F. Okino and H. Touhara, *Chem. Commun.*, 2005, 2002-2004.
31. N. F. Yudanov, A. V. Okotrub, Y. V. Shubin, L. I. Yudanova, L. G. Bulusheva, A. L. Chuvilin and J.-M. Bonard, *Chem. Mater.*, 2002, **14**, 1472-1476.
32. E. Unger, A. Graham, F. Kreupl, M. Liebau and W. Hoenlein, *Curr. Appl. Phys.*, 2002, **2**, 107-111.
33. K. S. Coleman, A. K. Chakraborty, S. R. Bailey, J. Sloan and M. Alexander, *Chem. Mater.*, 2007, **19**, 1076-1081.
34. H. Hu, B. Zhao, M. A. Hamon, K. Kamaras, M. E. Itkis and R. C. Haddon, *J. Am. Chem. Soc.*, 2003, **125**, 14893-14900.
35. J. L. Bahr and J. M. Tour, *J. Mater. Chem.*, 2002, **12**, 1952-1958.
36. I. Mazov, D. Krasnikov, A. Stadnichenko, V. Kuznetsov, A. Romanenko, O. Anikeeva and E. Tkachev, *Nanotechnology*, 2012, **2012**.
37. L.G.Bulusheva, A.V.Okotrub, E.Flahaut, I.P.Asanov, P.N.Gevko, V.O.Koroteev, Yu.V.Fedoseeva, A.Yaya and C.P.Ewels, *Chem. Mater.*, 2012, **24**, 2708
38. A. Rao, P. Eklund, S. Bandow, A. Thess and R. E. Smalley, *Nature*, 1997, **388**, 257-259.
39. G. Chen, S. Bandow, E. Margine, C. Nisoli, A. Kolmogorov, V. H. Crespi, R. Gupta, G. Sumanasekera, S. Iijima and P. Eklund, *Phys. Rev. Lett.*, 2003, **90**, 257403.
40. G. U. Sumanasekera, J. L. Allen, S. L. Fang, A. L. Loper, A. M. Rao and P. C. Eklund, *J. Phys. Chem. B*, 1999, **103**, 4292-4297.
41. G. Chen, C. Furtado, S. Bandow, S. Iijima and P. Eklund, *Phys. Rev. B: Condens. Matter*, 2005, **71**, 045408.
42. U. J. Kim, C. A. Furtado, X. Liu, G. Chen and P. C. Eklund, *J. Am. Chem. Soc.*, 2005, **127**, 15437-15445.
43. J. Coates, *Interpretation of infrared spectra, a practical approach*, 2000.